# NRC Publications Archive
# Archives des publications du CNRC

**Copper ion assisted photochemical vapor generation of chlorine for its sensitive determination by sector field inductively coupled plasma mass spectrometry**

Hu, Jing; Sturgeon, Ralph E.; Nadeau, Kenny; Hou, Xiandeng; Zheng, Chengbin; Yang, Lu

National Research Council Canada    Conseil national de recherches Canada

Canada

# Copper Ion Assisted Photochemical Vapor Generation of Chlorine for Its Sensitive Determination by Sector Field Inductively Coupled Plasma Mass Spectrometry

Jing Hu,[†,‡] Ralph E. Sturgeon,[‡] Kenny Nadeau,[‡] Xiandeng Hou,[*,†] Chengbin Zheng,[§] and Lu Yang[*,‡]

[†]Analytical & Testing Center, Sichuan University, 29 Wangjiang Road, Chengdu, Sichuan 610064, China
[‡]National Research Council Canada, 1200 Montreal Road, Ottawa, Ontario K1A 0R6, Canada
[§]Key Laboratory of Green Chemistry and Technology, and MOE College of Chemistry, Sichuan University, Chengdu, Sichuan 610064, China

**ABSTRACT:** A novel, reliable, and sensitive approach for the determination of chlorine by sector field inductively coupled plasma mass spectrometry (SF-ICPMS) using photochemical vapor generation for sample introduction is presented. Methyl chloride is generated from different chlorine species in a flow-through photochemical reactor using a 1% solution of acetic acid containing 7.5 $\mu g\ g^{-1}$ of $Cu^{2+}$. The volatile product is directed by an argon carrier gas to a gas–liquid separator and introduced into the instrument. A sample flow rate at 1.7 mL $min^{-1}$ and a 45 s irradiation time provided a 74-fold enhancement in sensitivity compared to conventional nebulization. A blank-limited detection limit of 0.5 ng $g^{-1}$ for chloride, suitable for quantitation at trace levels, was achieved. The proposed method was validated by analysis of two certified reference materials, NIST SRM 1568b rice flour and SRM 1571 orchard leaves, with satisfactory results, as well as three varieties of bottled water, achieving spike recoveries between 101% and 105%.
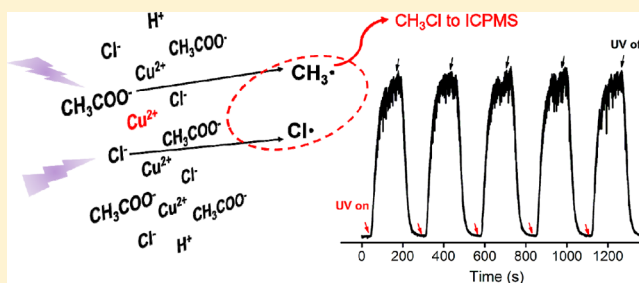
**C**hlorine, the most abundant halogen in the Earth's crust, is widely distributed in nature. As the most common form of chlorine, chloride is generally believed to cause no harm to the environment and living organisms, even at high levels. However, exposure to high concentrations of $Cl^-$ can cause severe corrosion of metallic pipes and increase the levels of metals in water.[1] Hence, chloride monitoring in environmental samples remains indispensable for quality control and management purposes. Moreover, in some cases, it is necessary to control the presence of chloride at trace levels. For instance, a maximum allowable $Cl^-$ level of 10 $\mu g\ L^{-1}$ has been established by the American Society for Testing and Materials (ASTM) for ultrapure water used in the production of devices in the electronics and semiconductor industries.[2] Other types of chlorine compounds, such as toxic hypochlorite and chloramine, widely used in water purification and disinfection, along with a variety of organic compounds such as polycyclic aromatic hydrocarbons (PAHs) and chlorinated solvents, are strictly regulated globally.[3−5]

Trace levels of chlorine are commonly determined by a few techniques, such as ion chromatography (IC),[6,7] neutron activation analysis (NAA),[8] X-ray fluorescence spectrometry,[9] inductively coupled plasma optical emission spectrometry (ICPOES),[10,11] and inductively coupled plasma mass spectrometry (ICPMS).[12−15] Recently, high-resolution continuum source graphite furnace molecular absorption spectrometry has been applied to the determination of chlorine via the formation of diatomic molecules such as $MgCl$,[16] $InCl$,[17] and $AlCl$.[18] Among these techniques, ICPMS has been often utilized for detection of chlorine.[19] Unfortunately, the determination of chlorine by ICPMS suffers potential spectral interferences arising from sample matrices and typical plasma gas species (e.g., $^{34}S^1H^+$, $^{19}F^{16}O^+$, $^{16}O^{18}O^1H^+$, $^{36}Ar^1H^+$, and $^{19}F^{18}O^+$), and it provides comparatively poor detection limits due to its high ionization potential (13.01 eV). Sector field ICPMS instruments have been adopted to address some of these issues;[14,20] interferences can be frequently eliminated, but the determination of Cl remains subject to memory effects when liquid introduction via nebulization is used. The reported detection limits are no better than 3 ng $g^{-1}$, even at high-resolution mode.[20]

It is well-known that the sample introduction efficiency for standard pneumatic nebulization is poor, typically ranging from 1 to 3% at a sample flow rate 1.0 mL $min^{-1}$. By contrast, chemical vapor generation (CVG), which transforms analytes of interest into their gaseous species, achieves significantly higher sample-introduction efficiency and is the subject of widespread research efforts.[21−24] Conventional CVG schemes utilizing tetrahydroborate reductant fail for the effective vapor
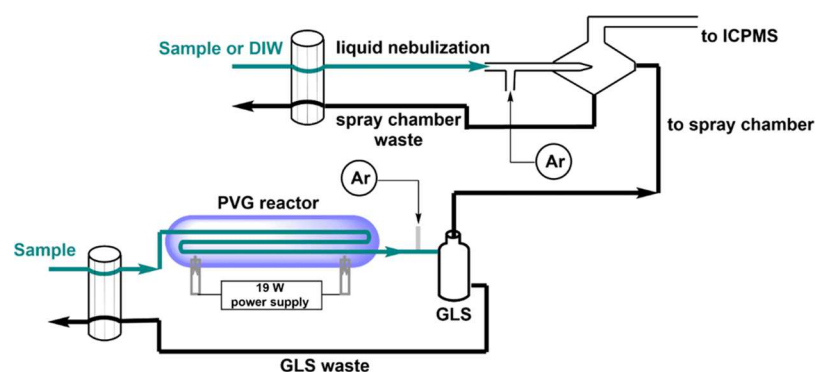
**Figure 1.** Schematic diagram of the UV-PVG system hyphenated to sector field ICPMS for vapor introduction of volatile chlorine species.

generation of transition metals and nonmetals, including halogens. Recent studies on photochemical vapor generation (PVG) have demonstrated its great potential for halogens.[25−31] Iodine was readily amenable to PVG, generating methyl iodide under UV irradiation of iodine in dilute acetic acid solution to yield an introduction efficiency of 94% for iodine and a 40-fold enhancement in sensitivity.[26] Bromine, in contrast, was not efficiently vapor-generable unless $NH_4Cl$ was present in a dilute solution of acetic acid.[27] Chlorine vapor generation appeared to be intractable under the above experimental conditions.

The aim of this study was to evaluate the feasibility of PVG of chlorine and develop a reliable, sensitive, and accurate method for its determination by a sector field ICPMS. A flow-through lamp rendering intense 185 nm UV irradiation was used for this purpose.

## EXPERIMENTAL SECTION

**Instrumentation.** All measurements were made using an Element XR (Thermo Fisher Scientific, Germany) sector field inductively coupled plasma mass spectrometer (SF-ICPMS). A combined cyclonic and Scott-type spray chamber allowing for simultaneous introduction of vapor-generated species and liquid nebulization was employed. A perfluoroalkoxy alkane (PFA) self-aspirating nebulizer (Elemental Scientific, Omaha, NE, U.S.A.) was used, operating at 230 $\mu$L min$^{-1}$.

A schematic diagram of the UV-PVG system hyphenated to SF-ICPMS is depicted in Figure 1. Sample solution was delivered at a nominal flow rate of 1.7 mL min$^{-1}$ to the PVG reactor using a Gilson Minipuls 2 peristaltic pump (Mandel Scientific, Villiers, Le Bel, France), which was also used to evacuate waste from the photochemical reaction. The PVG reactor comprised a 19 W low-pressure mercury discharge lamp (Beijing Titan instrument Co, Beijing, China), having a synthetic quartz central channel of ~700 $\mu$L volume. In this way, the sample solution was subjected to uniform and intense deep UV radiation while flowing through the photoreactor. The effluent was directed to a homemade gas−liquid separator (GLS, ~2 mL internal volume) supplied with a flow of argon gas via a Brooks model 5871-B mass flow controller (Emerson Electric Co., Hatfield, PA, U.S.A.). Volatile chlorine species from the GLS were then introduced to the inlet of the spray chamber for detection by SF-ICPMS.

UV−vis spectra of sample solutions were recorded with a Thermo Scientific Evolution 220 UV−visible spectrophotometer. A 5975C GC-MS from Agilent Technologies (Mississauga, ON, Canada) was used for identification of PVG products.

**Reagents and Materials.** Nitric acid was purified in-house by sub-boiling distillation of reagent-grade feedstock in a quartz still. ACS-grade sodium chloride and chloramine T, analytical-grade potassium chlorate, and 10−15% sodium hypochlorite solution were sourced from Fisher Scientific (Nepean, ON, Canada), BDH Chemicals, Ltd., (Poole, England), and Sigma-Aldrich Canada, Ltd. (Oakville, ON, Canada), respectively. High-purity ACS-grade glacial acetic, formic, and propionic acids were purchased from Fisher Scientific (Nepean, ON, Canada) and Sigma-Aldrich Canada, Ltd. (Oakville, ON, Canada). All solutions were prepared using high-purity deionized water (DIW) from a NanoPure mixed-bed ion-exchange system fed with reverse osmosis domestic feedwater (Barnstead/Thermolyne Corp, Dubuque, IA, U.S.A.). A solution of 10 000 $\mu$g g$^{-1}$ of Cu(II) was prepared by dissolving ultrahigh-purity copper wire (99.999%, ESPI Metals, Ashland, OR, U.S.A.) in a few mL of double-distilled nitric acid and diluting with DIW. Anhydrous sodium carbonate (analytical grade, >99.9%) and zinc oxide (99.9%, 200-mesh powder) were obtained from BDH Chemicals Ltd. (Poole, England) and Alfa Aesar (Ward Hill, MA, U.S.A.), respectively. Analytical-grade phosphoric acid (Anachemia Chemicals) and a 1 M solution of sodium hydroxide (ACS grade, Fisher Scientific) were used for pH adjustment of test solutions prior to PVG. A 5% $NH_3 \cdot H_2O$ (v/v) rinse solution was prepared and used between samples to minimize memory effects via liquid nebulization.

Two certified reference materials, NIST 1568b rice flour and 1571 orchard leaves, were used for method validation. The accuracy of the methodology was also verified based on spike recovery tests from three suppliers of bottled water purchased from a local supermarket.

**Sample Preparation and Analytical Procedure.** For NIST 1568b rice flour and 1571 orchard leaves, a sintering sample-preparation method was adopted following the procedure of Österlund et al.[14] Sintering reagent was prepared by mixing 45 g of $Na_2CO_3$ and 30 g of ZnO. Nominal 0.3 g subsamples were weighed into precleaned ceramic crucibles and completely covered by 0.75 g of sintering reagent, followed by sintering in a muffle furnace at 560 °C for 2 h. After cooling down, the residue was transferred to clean screw-capped polypropylene bottles and dissolved in 30 g of DIW. The solutions were allowed to stand overnight at room temperature to ensure maximum dissolution. A subsample of the supernatant was diluted 50-fold with 1% (v/v) solution of acetic acid spiked to contain 7.5 $\mu$g g$^{-1}$ Cu(II) for analysis by the method of additions when using PVG sample introduction. Subsamples of 10 g were spiked to result in approximately 0.5-, 1.0-, 2.0-, and 3.0-fold increases in the concentration of chloride in the prepared samples. Dry weights of all samples were corrected for

moisture content by subtraction of the mass difference after drying for 4 h at 85 °C.

Triplicate 50 g masses of bottled demineralized water samples were spiked with acetic acid (HAc) and Cu(II) to provide a solution containing 1% HAc and 7.5 $\mu$g g$^{-1}$ Cu(II). Subsamples of 10 g of this solution were then spiked with a Cl standard to yield test solutions containing approximately 0.5-, 1.0-, 2.0-, and 3.0-fold increases in their estimated concentration of chloride and used for calibration by the method of additions. Natural spring water samples were diluted 200-fold with DIW and then subjected to the same sample-preparation procedure outlined above.

Optimization of the SF-ICPMS instrument was undertaken daily using nebulization of a 1 ppb (ng g$^{-1}$) multielement tuning solution in the absence of PVG sample introduction. When PVG was in use, nebulization of DIW was continued and the Ar carrier gas flow was optimized for maximum sensitivity for $^{35}$Cl in a 100 ng g$^{-1}$ solution of chloride in 1% acetic acid containing 10 $\mu$g g$^{-1}$ of Cu(II). Typical operating conditions are summarized in Table 1. The $^{35}$Cl isotope was monitored in

**Table 1. SF-ICPMS ElementXR Operating Conditions**

| | |
|---|---|
| Rf power | 1167 W |
| plasma Ar gas flow rate | 16.0 L min$^{-1}$ |
| auxiliary Ar gas flow rate | 1.00 L min$^{-1}$ |
| nebulizer Ar gas flow rate | 1.10 L min$^{-1}$ |
| Ar carrier gas flow rate to GLS | 0.12 L min$^{-1}$ |
| sampler cone orifice (nickel) | 1.00 mm |
| skimmer cone orifice (nickel) | 0.88 mm |
| lens voltage | focus, −990 V; x deflection, −3.60 V; y deflection, 3.30 V; shape, 115 V; Quad1, 0 V (LR) |
| SEM | 1650 V |
| Faraday deflection | −209 V |
| dead time | 25 ns |
| resolution | LR ≈ 300 |
| data acquisition | E-scan, 5% mass window; 0.015 s sample time, 150 samples per peak; 700 runs and 1 pass; 80% integration window |

analog mode after steady-state signals were achieved using PVG sample introduction over the course of 180 s of sample uptake time. Unless otherwise specified, all measurements were undertaken at low-resolution mode with a total 85 s measurement time.

Relative response from PVG of different chlorine species, including chloride, hypochlorite, chlorate, and chloramine T, was studied based on 2 $\mu$g g$^{-1}$ working solutions of each of these compounds. Concentrations of hypochlorite, chlorate, and chloramine T were calibrated against the chloride standard solution, assuming that nebulization of solutions of all chlorine compounds provided equivalent response.

To identify the gaseous product of PVG of Cl, volatile chlorine species from the photochemical reaction were collected using the method described by Sturgeon et al.[27] The gas phase was directed by a stream of Ar from the outlet of the GLS to a clean, Ar-flushed 500 mL glass cylinder fitted with stopcocks at both ends and a septum port in the center. A 1000 $\mu$g g$^{-1}$ solution of chloride in 1% acetic acid containing 7.5 $\mu$g g$^{-1}$ Cu(II) was continually pumped through the photoreactor, allowing the volatile chlorine species to flush and fill the gas sampling bulb. After several minutes, the stopcocks were closed. A 500 $\mu$L aliquot of the product was taken with a gas sampling

syringe via the septum port and injected into the GC-MS. The inlet temperature was 200 °C with injection performed in split mode (10:1). A DB-5.625 column (5% phenyl−95% dimethylpolysiloxane, 30 m × 0.25 mm i.d. × 0.25 $\mu$m film thickness) was held at 35 °C for 10 min with a He carrier gas flow of 1 mL min$^{-1}$. The mass spectrum was acquired over an $m/z$ range 35−150 with electron energy (EI) set at 70 eV.

*Safety Considerations.* The photochemically generated chlorine species were identified as highly toxic methyl chloride. Cautious handling, personal protection, and proper ventilation during all manipulations should be employed.

## ■ RESULTS AND DISCUSSION

**Optimization of UV-PVG.** Despite successful PVG of iodine[26] and bromine[27] in acetic acid or acetic acid containing NH$_4$Cl, use of similar conditions was unsuccessful for the PVG of chlorine. Studies by Bakač[32] and Carraher et al.[33] suggested that halide ions greatly accelerate the photochemical reaction between transition metal ions and alkyl radicals to generate volatile alkyl halides. A preliminary attempt demonstrated that PVG of Cl$^-$ was achievable in the presence of a few hundred ppm ($\mu$g g$^{-1}$) of Fe$^{3+}$ or several ppm of Cu$^{2+}$. The significance of this observation will be discussed later (Transition Metal Ion Assisted UV-PVG section). As Cu(II) was found to be more efficient in assisting PVG of Cl$^-$, it was selected for further study and optimization.

Under optimal instrumental conditions, a suite of experimental parameters affecting PVG of Cl$^-$ was further investigated to yield maximum response, including low-molecular-weight organic acid type and concentration, pH of the generation solution, sample flow rate (irradiation time), and concentration of Cu$^{2+}$. The influence of sample pH was examined first. Standard solutions of 50 ng g$^{-1}$ of Cl$^-$, prepared in 1% acetic acid containing 10 $\mu$g g$^{-1}$ of Cu and adjusted over a pH range 1.7−3.7 using H$_3$PO$_4$ or NaOH, were investigated. For these experiments, an arbitrary sample flow rate to the photoreactor of 1.2 mL min$^{-1}$ and the optimized Ar carrier flow rate of 0.12 L min$^{-1}$ to the GLS were used. As evident in Figure 2A, high and constant responses were obtained when the sample pH was between 1.8 and 2.3, whereas decreased response was observed at both lower and higher pH values. Note that the pH of 1% (v/v) acetic acid is 2.2.

Similarly, the effect of acetic acid concentration was evaluated with use of a sample flow rate of 1.7 mL min$^{-1}$ to the photoreactor and an Ar carrier gas flow rate of 0.12 L min$^{-1}$. The concentration of Cu$^{2+}$ in the sample was fixed at 10 $\mu$g g$^{-1}$. As shown in Figure 2B, 1% (v/v) acetic acid generated the highest response. For simplicity, as the pH of 1% (v/v) acetic acid is ∼2.2, no further pH adjustment was used for all subsequent experiments.

Only PVG of Cl$^-$ in formic and propionic acid media was investigated as well. It was found that the presence of even 0.1% formic acid in the 1% acetic acid solution led to an almost 60% decrease in $^{35}$Cl intensity. In the presence of 1% propionic acid, the resultant $^{35}$Cl response was merely 0.4% of that from pure 1% acetic acid. In accordance with the generally accepted free radical mechanism of PVG,[34] it is speculated that formic acid may generate water-soluble HCl, which remains in the solution, whereas propionic acid may produce ethyl chloride having much lower volatility. When acetic acid was used, the PVG-generated species was found to be methyl chloride, as confirmed by GC-MS analysis of the collected product, as shown in Figure 3.
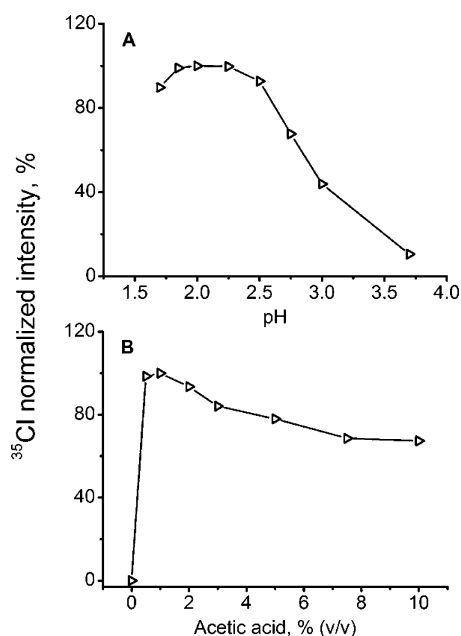
**Figure 2.** Effect of (A) pH of sample solution and (B) concentration of acetic acid on relative responses from 50 ng g$^{-1}$ of Cl$^-$ standard solutions containing 10 $\mu$g g$^{-1}$ of Cu$^{2+}$ in 1% acetic acid (A) and various amount of acetic acid (B), respectively, using PVG sample introduction.
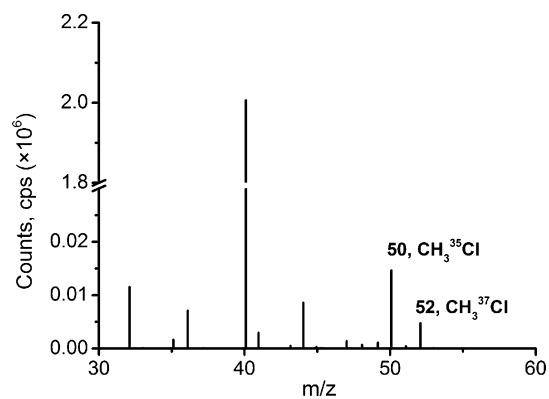


**Figure 3.** GC-MS spectrum of the headspace gas containing the reaction products from photochemical vapor generation of a 1000 $\mu$g g$^{-1}$ chloride solution in 1% (v/v) acetic acid containing 7.5 $\mu$g g$^{-1}$ of Cu$^{2+}$.

Sample delivery rate determines both the amount of analyte supplied to the PVG reactor and the irradiation time. The effect of sample delivery rate was studied over a wide range, from 0.2−6.4 mL min$^{-1}$. As shown in Figure 4, a near linear increase in $^{35}$Cl intensity is observed for sample delivery rates in the range of 0.2−1.0 mL min$^{-1}$, indicating that the efficiency of the generation and transport system is constant under these conditions. Optimal response was achieved at a delivery rate of 1.4−2.2 mL min$^{-1}$ and then decreased at higher transport flow rates, likely due to either insufficient irradiation time or compromised performance of the GLS device. A sample delivery rate of 1.7 mL min$^{-1}$, corresponding to ∼45 s irradiation time, was selected for all subsequent measurements.

**Transition Metal Ion Assisted UV-PVG.** As reported in recent studies, the presence of several metal ions[28,35] or specific reagents[27] may serve as sensitizers that significantly enhance PVG efficiency for a number of analytes. Studies by Bakač[32]
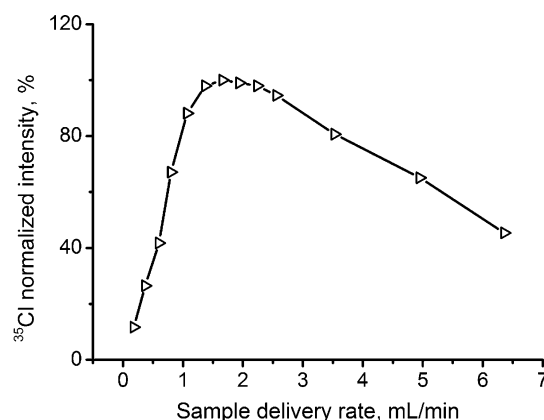


**Figure 4.** Impact of sample delivery rate on relative response from a 50 ng g$^{-1}$ of Cl$^-$ using PVG sample introduction.

and Carraher et al.[33] suggest that halide ions greatly accelerate the photochemical reaction between transition metal ions and alkyl radicals for the generation of volatile alkyl halides. Correspondingly, transition metal ions such as Fe(III) and Cu(II) may enhance the efficiency of photochemical production of chloride species. To confirm this, standard solutions of Cl$^-$ prepared in 1% HAc solution were spiked with varying amounts of ultrapure solutions of these potential "sensitizers", including Ni(II), Co(II), Mn(II), Zn(II), Fe(III), Cu(II), and NH$_4$Ac. It was found that Ni(II), Co(II), Mn(II), and Zn(II), even at as high as 150 $\mu$g g$^{-1}$ level, and up to 2000 $\mu$g g$^{-1}$ NH$_4$Ac, were incapable of inducing PVG of Cl$^-$. However, a few hundred $\mu$g g$^{-1}$ of Fe(III) slightly enhanced the PVG whereas Cu(II) was found to be the most effective for improving the signal. As shown in Figure 5, chloride was not
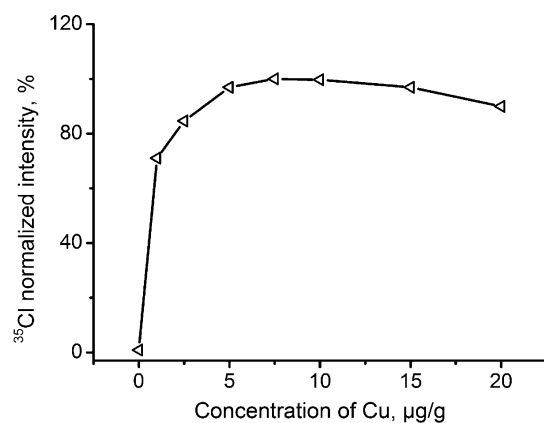


**Figure 5.** Effect of Cu(II) concentration on relative response from 50 ng g$^{-1}$ Cl$^-$ solutions in 1% acetic acid using PVG sample introduction.

vapor-generable in the absence of Cu(II). PVG response from a 50 ng g$^{-1}$ Cl standard increased remarkably as Cu(II) concentration increased from 0 to 5 $\mu$g g$^{-1}$, remained constant up to 10 $\mu$g g$^{-1}$, and thereafter slightly decreased at higher values. Consequently, 7.5 $\mu$g g$^{-1}$ of Cu(II) was selected for all subsequent measurements in consideration of maximum response being achieved at minimum concentration.[36]

As noted earlier, the photochemically generated species of Cl$^-$ was confirmed to be CH$_3$Cl by GC-MS detection (Figure 3). This observation is consistent with the ligand-to-metal charge transfer (LMCT) model discussed by Sturgeon in recent reviews on mechanisms of PVG[34,36] and the radical-mediated

halogen atom abstraction process proposed by Bakač[32] and Carraher et al.,[33] wherein the formation of complexes of transition metal ions with carboxylic acid and halide ions may serve as immediate species for the photochemical reaction to proceed further. Thus, it may be speculated that the formation of metal carboxylates and photochemical reaction efficiency of chloride should depend on the pH of the solution. As expected, a few microliters of concentrated nitric acid to adjust to proper pH range was found to be indispensable for the generation of $CH_3Cl$ in our preliminary experiments with use of Fe(III) as modifier, whereas for Cu(II) the same amount of nitric acid induced severe suppression of Cl response. More interestingly, noticeable variations in the photoabsorption spectrum of the sample solutions measured by a UV−visible spectrophotometer emerged as well, as evident in Figure 6. Specifically, addition of
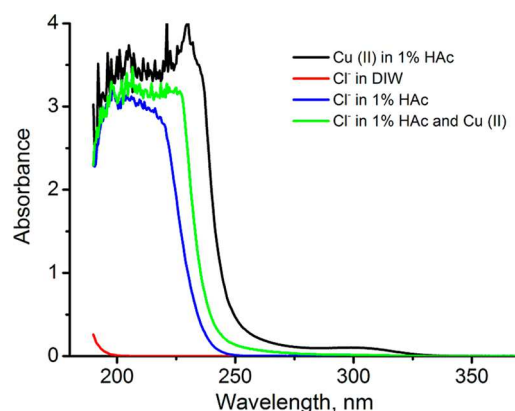


**Figure 6.** UV−vis spectra of various test solutions: the concentrations of $Cl^-$ and Cu(II) in the test solutions were 10 and 20 $\mu g\ g^{-1}$, respectively.

Cu(II) to 1% (v/v) acetic acid solution resulted in the appearance of new LMCT bands starting from low energy around 325 nm. The presence of chloride, however, led to an obvious shift of the onset of this band to 280 nm but still differed from that of 1% acetic acid solution (250 nm). Presumably, Cu(II) served as a "sensitizer" for the photoreaction via accelerated decarboxylation of the acetic acid[33] as a result of enhanced absorption evident at the principal discharge line of 254 nm emanating from the low-pressure Hg lamp comprising the photoreactor.

**Influence of Transition Metals and $HNO_3$ on the PVG of Cl.** Transition metals and $NO_3^-$ often have adverse effects on the PVG of many analytes;[30] their effects on the responses from Cl were also investigated. Results are summarized in Table 2. It is evident that none of the transition metals of interest ($Mn^{2+}$, $Zn^{2+}$, $Ni^{2+}$, $Co^{2+}$, $Fe^{3+}$, and $Cr^{VI}$) displayed significant improvement or suppression of signals, except a 10 $\mu g\ g^{-1}$ $Zn^{2+}$ spiked solution showed a slight enhancement. Although a few hundred $\mu g\ g^{-1}$ of Fe(III) alone was found to facilitate PVG of Cl, as demonstrated above, the addition of 1−10 $\mu g\ g^{-1}$ Fe(III) to the generation solution containing 7.5 $\mu g\ g^{-1}$ Cu(II) could not yield higher response, either because the amount of spiked Fe(III) was inadequate to induce a synergistic enhancement or because the PVG condition used was optimal for Cu(II) modifier but was not the best for Fe(III). Furthermore, as reported in previous studies, nitrate ions were detrimental to the PVG efficiency. Not surprisingly, the presence of 15 mM $NO_3^-$ led to a remarkable 40% decrease in

**Table 2. Relative Effects of Added Transition Metals and $NO_3^-$ on PVG of Cl**

| element | amount added, $\mu g\ g^{-1}$ (mM) | signal intensity ratio[a] |
|---|---|---|
| $Mn^{2+}$ | 5 | 1.04 |
| | 10 | 1.08 |
| $Zn^{2+}$ | 5 | 1.04 |
| | 10 | 1.27 |
| $Ni^{2+}$ | 5 | 1.14 |
| | 10 | 1.04 |
| $Co^{2+}$ | 5 | 1.02 |
| | 10 | 1.03 |
| $Fe^{3+}$ | 1 | 1.07 |
| | 5 | 1.08 |
| | 10 | 1.10 |
| Cr(VI) | 5 | 1.08 |
| | 10 | 1.10 |
| $NO_3^-$ | (7.5) | 0.92 |
| | (15) | 0.59 |

[a]Ratio of response obtained from 0.050 $\mu g\ g^{-1}$ standard solutions of $Cl^-$ in 1% HAc and 7.5 $\mu g\ g^{-1}$ $Cu^{2+}$ with addition of various amounts of interference ions to the response from a pure 0.050 $\mu g\ g^{-1}$ standard solution of $Cl^-$ in 1% HAc and 7.5 $\mu g\ g^{-1}$ $Cu^{2+}$.

the response of PVG of $Cl^-$. However, a merely 8% decrease was noted with 7.5 mM $NO_3^-$, suggesting that PVG of $Cl^-$ should be tolerant to nitrate ions to some extent and should suffer negligible impact from nitrate after the addition of 0−20 $\mu L$ Cu(II) modifier from 10 000 $\mu g\ g^{-1}$ Cu(II) stock (prepared from dissolution of copper wire in 5% $HNO_3$) to the sample solution.

**Analytical Performance.** Steady-state PVG signals could be generated over the course of a 85 s sample introduction period, which were then used for quantitation or comparison of relative analytical performance throughout this work. PVG responses from different forms of chlorine, including chloride, hypochlorite, chloramine T, and chlorate, were compared under optimized experimental conditions. As presented in Figure 7, the relative response from these chlorine species differ, suggesting varied kinetics or mechanisms of the reactions. UV−vis spectra of the various solutions tested were not acquired. Vapor generation efficiencies follow the order chloride > chloramine T > chlorate > hypochlorite.

Using chloride as an example, analytical figures of merit are summarized in Table 3, which highlight the advantages of PVG
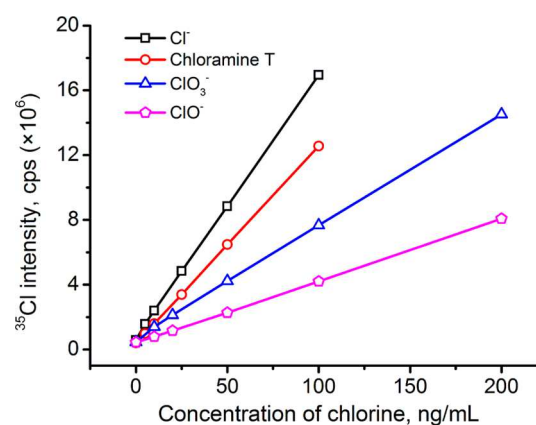


**Figure 7.** PVG response from individual standard solutions of $Cl^-$, $ClO_3^-$, $ClO^-$, and chloramine T.

**Table 3. Figures of Merit**

| | low resolution | | high resolution | |
|---|---|---|---|---|
| | PVG sampling | nebulization | PVG sampling | nebulization |
| precision, % RSD @ 50 ng g$^{-1}$ | 1.7 | 4.9 | 1.9 | 6.8 |
| LOD$^a$, ng g$^{-1}$ | 0.46 | 6.8 | 0.45 | 6.7 |
| blank$^b$, ng g$^{-1}$ | 4.3 | | 3.8 | |
| PVG efficiency$^c$ | 80 | | | |
| linear range, ng g$^{-1}$ | 2–500 with $R^2$ of 0.999 | | 2–500 with $R^2$ of 0.999 | |

$^a$On the basis of 3 times the standard deviation of the method blank ($n = 7$). $^b$For $^{35}$Cl, based on standard additions analysis of the generation medium comprising 1% acetic acid in deionized water containing 7.5 $\mu$g g$^{-1}$ of Cu(II). $^c$On the basis of response from PVG sampling of Cl$^-$ relative to that from solution nebulization, assuming the introduction efficiency of the latter at 0.23 mL/min sample uptake rate was 8%.[37]

sample introduction over direct solution nebulization. Under optimized experimental conditions, a 74-fold enhancement in sensitivity is realized using PVG. In addition, the severe memory effect encountered during pneumatic nebulization was completely eliminated with PVG sample introduction to the ICPMS. Unfortunately, a relatively high blank of ∼4 ng g$^{-1}$ was inevitably encountered even when ultrapure DIW and reagents were used. As a result, the limit of detection (LOD) of the proposed PVG method is compromised and values of 0.46 and 0.45 ng g$^{-1}$ were obtained at low and high resolution, respectively, based on three times the standard deviation of method blanks using external calibration. Despite this drawback, a 15-fold improvement in LOD was obtained. A precision of <2% RSD for replicate measurements of 50 ng g$^{-1}$ chloride was obtained using PVG sampling. The 74-fold increase in sensitivity with PVG suggests that the overall efficiency (generation, phase separation, and transport) compared to pneumatic nebulization (assumed to be nominally 8%[37] and accounting for the 1.7 mL/min PVG sample flow rate vs 0.23 mL min$^{-1}$ for nebulization) is 80%. The linear range of the proposed method runs from 2 to 500 ng g$^{-1}$ Cl with $R^2$ of 0.999, as summarized in Table 3.

**Method Validation and Applications to Water Samples.** Standard additions calibration was employed for quantitation under optimized experimental conditions to achieve final accurate results. As a result of PVG sample introduction, potential spectral interferences arising from sample matrices (e.g., $^{34}$S$^1$H$^+$, $^{19}$F$^{16}$O$^+$, and $^{19}$F$^{18}$O$^+$) are minimized. The high blank encountered arises mainly from DIW and not from spectral interferences, because similar values of blank were obtained at low and high resolution, respectively. Because analytical performance is similar between low and high resolution, for simplicity, low resolution was used for the final quantitation of chlorine. By sintering the two reference materials, all forms of chlorine were converted to HCl(g) and quantitatively trapped by Na$_2$CO$_3$ in the sintering agent,[14] and thus were present as chloride in the prepared sample solutions:

$$2HCl(g) + Na_2CO_3(s)$$
$$\rightarrow 2NaCl(s) + H_2O(g) + CO_2(g) \quad (1)$$
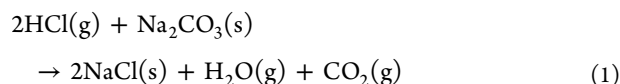
Appropriate amounts of Cl$^-$ standard solution were added to prepare test samples so as to result in 1-, 2-, and 4-fold increases in the expected concentrations of chloride. The Cu(II) sensitizer was added to all solutions (7.5 $\mu$g g$^{-1}$ of Cu) to enhance the response. Method blanks arising from the sintering agents were quantitated in the same way, and their content was subtracted from total concentrations measured in the reference materials. Analytical results obtained from three replicate measurements of each reference material are summarized in

Table 4. The determined total Cl concentrations in the two reference materials are in agreement with the certified (for

**Table 4. Analytical Results**

| sample | determined | certified (reference) value | spike recovery (%) |
|---|---|---|---|
| no. 1 bottled water (ng g$^{-1}$) | 56.2 | | 101 |
| no. 2 bottled water (ng g$^{-1}$) | 120 | | 105 |
| no. 3 bottled water ($\mu$g g$^{-1}$) | 21.3 | | 100 |
| NIST 1568b ($\mu$g g$^{-1}$) | 301.9 ± 11.4 | 301.1 ± 3.8 | |
| NIST 1571 ($\mu$g g$^{-1}$) | 644.9 ± 14.2 | (690) | |

NIST 1568b) or reference (for NIST 1571) values, demonstrating the accuracy and reliability of the proposed method.

Three bottled waters were analyzed and spike-recovery tests were performed at the analyte concentration levels determined in each sample, assuming that the major chlorine species in each bottled water was chloride.[38] As evident from Table 4, spike recoveries of 101%–105% were achieved. Demineralized waters that underwent multistep purification (sample nos. 1 and 2) contain significantly lower Cl than naturally sourced spring water (sample no. 3). Applications to other water matrices were not attempted because responses from different chlorine species are significantly different. Such applications were deemed beyond the scope of the present study. Nevertheless, it is evident that speciation could be readily achieved by coupling sample processing with ion chromatography for initial species separation and directing the effluent to the PVG reactor for quantitation after online addition of acetic acid and Cu(II) sensitizer. A multispecies calibration standard, similarly treated, would resolve this issue satisfactorily.

## ■ CONCLUSIONS

A novel, reliable, and sensitive approach for the determination of chlorine was developed using PVG for sample introduction and SF-ICPMS for detection. Under optimized experimental conditions, a blank-limited detection limit of 0.5 ng g$^{-1}$ as chloride and a 74-fold enhancement in sensitivity compared to that with pneumatic nebulization were obtained as a consequence of an estimated 80% overall introduction efficiency. Featuring simplicity, low consumption of reagents, and lower memory effect, the proposed methodology has potential for monitoring trace-level chloride, such as in ultrapure water used in the electronics and semiconductor industries, and confirmation of the stoichiometry of chlorinated organic compounds.

Photochemical vapor generation of $CH_3Cl$ from various chlorine compounds can be achieved in a dilute acetic acid medium containing Cu(II) as a sensitizer or PVG accelerant. The role of Cu(II) and the impact on PVG efficiencies of the various chlorine species are not clear at this time, and further investigations are needed to improve our understanding of this technique. Nevertheless, this presents no impediment to the utilization of PVG for analytical purposes. The successful determination of chlorine in two CRMs and various bottled waters validates the methodology for application to real sample analysis.

## ■ AUTHOR INFORMATION

**Corresponding Authors**
*houxd@scu.edu.cn.
*Lu.yang@nrc-cnrc.gc.ca.
**ORCID**
Lu Yang: 0000-0002-6896-8603
**Notes**
The authors declare no competing financial interest.

## ■ ACKNOWLEDGMENTS

## ■ REFERENCES

(1) Yakoh, A.; Rattanarat, P.; Siangproh, W.; Chailapakul, O. *Talanta* **2018**, *178*, 134−140.

(2) ASTM D5127-13. *Standard Guide for Ultra-Pure Water Used in the Electronics and Semiconductor Industries*; ASTM International: West Conshohocken, PA, 2013; DOI: 10.1520/D5127-13.

(3) Richardson, S. D.; Ternes, T. A. *Anal. Chem.* **2014**, *86*, 2813−2848.

(4) Postigo, C.; Richardson, S. D. *J. Hazard. Mater.* **2014**, *279*, 461−475.

(5) Moran, M. J.; Zogorski, J. S.; Squillace, P. J. *Environ. Sci. Technol.* **2007**, *41*, 74−81.

(6) Noguchi, Y.; Zhang, L.; Maruta, T.; Yamane, T.; Kiba, N. *Anal. Chim. Acta* **2009**, *640*, 106−109.

(7) Colaruotolo, J. F.; Eddy, R. S. *Anal. Chem.* **1977**, *49*, 884−885.

(8) Chang, H. P.; Meric, I.; Sudac, D.; Nad, K.; Obhođas, J.; Gardner, R. P. *Fuel* **2017**, *209*, 643−649.

(9) Vander Hoogerstraete, T.; Jamar, S.; Wellens, S.; Binnemans, K. *Anal. Chem.* **2014**, *86*, 3931−3938.

(10) Nunes, T. S.; Muller, C. C.; Balestrin, P.; Muller, A. L. H.; Mesko, M. F.; Mello, P. d. A.; Muller, E. I. *Anal. Methods* **2015**, *7*, 2129−2134.

(11) Nakata, K.; Hashimoto, B.; Uchihara, H.; Okamoto, Y.; Ishizaka, S.; Fujiwara, T. *Talanta* **2015**, *138*, 279−284.

(12) Balcone-Boissard, H.; Michel, A.; Villemant, B. *Geostand. Geoanal. Res.* **2009**, *33*, 477−485.

(13) Date, A. R.; Stuart, M. E. *J. Anal. At. Spectrom.* **1988**, *3*, 659−665.

(14) Österlund, H.; Rodushkin, I.; Ylinenjärvi, K.; Baxter, D. C. *Waste Manage. (Oxford, U. K.)* **2009**, *29*, 1258−1264.

(15) de Gois, J. S.; Pereira, É. R.; Welz, B.; Borges, D. L. G. *Anal. Chim. Acta* **2014**, *852*, 82−87.

(16) Medeiros, R. L. d. S.; Souza, S. O.; Araújo, R. G. O.; da Silva, D. R.; Maranhão, T. d. A. *Talanta* **2018**, *176*, 227−233.

(17) Machyňák, L.; Čacho, F.; Němeček, M.; Beinrohr, E. *Spectrochim. Acta, Part B* **2016**, *125*, 140−145.

(18) Fechetia, M.; Tognon, A. L.; da Veiga, M. A. M. S. *Spectrochim. Acta, Part B* **2012**, *71−72*, 98−101.

(19) Mello, P. A.; Barin, J. S.; Duarte, F. A.; Bizzi, C. A.; Diehl, L. O.; Muller, E. I.; Flores, E. M. M. *Anal. Bioanal. Chem.* **2013**, *405*, 7615−7642.

(20) Bu, X.; Wang, T.; Hall, G. *J. Anal. At. Spectrom.* **2003**, *18*, 1443−1451.

(21) Gao, Y.; Liu, R.; Yang, L. *Chin. Sci. Bull.* **2013**, *58*, 1980−1991.

(22) Wu, P.; He, L.; Zheng, C.; Hou, X.; Sturgeon, R. E. *J. Anal. At. Spectrom.* **2010**, *25*, 1217−1246.

(23) Pohl, P.; Prusisz, B. *Anal. Bioanal. Chem.* **2007**, *388*, 753−762.

(24) Guo, X.; Sturgeon, R. E.; Mester, Z.; Gardner, G. J. *Anal. Chem.* **2004**, *76*, 2401−2405.

(25) Zheng, C.; Yang, L.; Sturgeon, R. E.; Hou, X. *Anal. Chem.* **2010**, *82*, 3899−3904.

(26) Grinberg, P.; Sturgeon, R. E. *J. Anal. At. Spectrom.* **2009**, *24*, 508−514.

(27) Sturgeon, R. E. *Anal. Chem.* **2015**, *87*, 3072−3079.

(28) Gao, Y.; Xu, M.; Sturgeon, R. E.; Mester, Z.; Shi, Z.; Galea, R.; Saull, P.; Yang, L. *Anal. Chem.* **2015**, *87*, 4495−4502.

(29) Gao, Y.; Li, S.; He, H.; Li, T.; Yu, T.; Liu, R.; Ni, S.; Shi, Z. *Microchem. J.* **2017**, *130*, 281−286.

(30) Zheng, C.; Sturgeon, R. E.; Brophy, C. S.; He, S.; Hou, X. *Anal. Chem.* **2010**, *82*, 2996−3001.

(31) Gao, Y.; Sturgeon, R. E.; Mester, Z.; Pagliano, E.; Galea, R.; Saull, P.; Hou, X.; Yang, L. *Microchem. J.* **2016**, *124*, 344−349.

(32) Bakač, A. *Croat. Chem. Acta* **2001**, *74*, 633−640.

(33) Carraher, J. M.; Pestovsky, O.; Bakac, A. *Dalton Trans.* **2012**, *41*, 5974−5980.

(34) Sturgeon, R. E. *J. Anal. At. Spectrom.* **2017**, *32*, 2319−2340.

(35) Wang, Y.; Lin, L.; Liu, J.; Mao, X.; Wang, J.; Qin, D. *Analyst* **2016**, *141*, 1530−1536.

(36) Sturgeon, R. E.; Grinberg, P. *J. Anal. At. Spectrom.* **2012**, *27*, 222−231.

(37) Olesik, J. W. Inductively Coupled Plasma Mass Spectrometers. In *Treatise on Geochemistry*, 2nd ed.; Turekian, K. K., Ed.; Elsevier: Oxford, U.K., 2014; pp 309−336.

(38) Foltz, F. *Bull. Sci. Technol. Soc.* **1999**, *19*, 300−309.